**The EMBO Journal** Vol. 22 No. 3 pp. 450–458, 2003

# A conserved tyrosine in the neck of a fungal kinesin regulates the catalytic motor core

**Friederike Schäfer, Dominga Deluca[1], Ulrike Majdic, Joachim Kirchner, Manfred Schliwa, Luis Moroder[1] and Günther Woehlke[2]**

Adolf Butenandt Institute, Cell Biology, University of Munich, Schillerstraße 42, D-80336 Munich and [1]Max Planck Institute for Biochemistry, Department of Bioorganic Chemistry, Am Klopferspitz 18a, D-82152 Martinsried, Germany

[2]Corresponding author
e-mail: guenther.woehlke@lrz.uni-muenchen.de

**The neck domain of fungal conventional kinesins displays characteristic properties which are reflected in a specific sequence pattern. The exchange of the strictly conserved Tyr 362, not present in animals, into Lys, Cys or Phe leads to a failure to dimerize. The destabilizing effect is confirmed by a lower coiled-coil propensity of mutant peptides. Whereas the Phe substitution has only a structural effect, the Lys and Cys replacements lead to dramatic kinetic changes. The steady state ATPase is 4- to 7-fold accelerated, which may be due to a faster microtubule-stimulated ADP release rate. These data suggest that an inhibitory effect of the fungal neck domain on the motor core is mediated by direct interaction of the aromatic ring of Tyr 362 with the head, whereas the OH group is essential for dimerization. This is the first demonstration of a direct influence of the kinesin neck region in regulation of the catalytic activity.**

*Keywords*: ATPase kinetics/conventional kinesin/dimerization/neck domain/synthetic peptides

## Introduction

The filamentous fungus *Neurospora crassa* possesses an unusually fast kinesin (NcKin) (Steinberg and Schliwa, 1996). Judged from the sequence homology, NcKin is a conventional kinesin with the same domain organization as its animal relatives (Steinberg, 1998). The N-terminal heads are responsible for microtubule binding and ATP hydrolysis, and thus constitute the catalytic core of the motor. The following ~10 amino acids form the flexible neck linker, which is thought to couple the enzymatic events in the head during movement. The subsequent domain, the neck, forms a coiled-coil, and, at least in animal kinesins, is sufficient for dimerization. Further towards the C-terminal, a flexible hinge domain joins the motility-generating N-terminus parts of the molecule to the stalk and tail domains, which are important for cargo-binding and regulation (Kozielski *et al*., 1997; Vale and Fletterick, 1997; Woehlke and Schliwa, 2000).

Truncated animal conventional kinesins lacking the neck are unable to dimerize. They usually behave as non-processive motors that are slower than their dimeric counterparts (Jiang and Hackney, 1997; Young *et al*., 1998). All conventional kinesins characterized so far seem to be processive, which means that they make many consecutive steps along the microtubule before dissociating. It is thought that the two heads of the heavy-chain dimer must interact to drive processive movement (Ma and Taylor, 1997a,b; Hancock and Howard, 1999). They bind to the filament in an alternating fashion and in this way drive stepwise movement. This mechanism requires coordination between the heads, which presumably is mediated by the neck domain. In agreement with this, an internal deletion of the neck region in the fungal kinesin from *Syncephalastrum racemosum* leads to uncoupling of gliding and ATP hydrolysis (Grummt *et al*., 1998). In the deletion mutant, gliding is slowed 3-fold whereas the catalytic activity is accelerated 5-fold. Conversely, alterations of the neck domain that do not interfere with the propensity of the neck to form a coiled-coil structure have relatively little effect on the motile properties of the motor (Romberg *et al*., 1998). Based on findings such as these, the neck is generally believed to serve as a dimerization domain that plays an indirect passive role in processive movement. Recently, it was suggested that the neck domain may be important for determining the run length of conventional kinesins (Thorn *et al*., 2000). The processivity of kinesin could be increased by introducing positive charges in the neck coiled-coil, whereas the introduction of negatively charged residues resulted in a decreased run length.

Because the dominant functional property of the neck of animal conventional kinesins is its ability to dimerize, monomeric constructs including the neck domain do not exist (Huang *et al*., 1994; Jiang *et al*., 1997) and, so far, other functions associated with this domain have not been discovered. However, constructs comprising the motor domain, neck linker and neck in NcKin are monomeric (Kallipolitou *et al*., 2001). This interesting fact indicates that the necks of fungal kinesins have different dimerization properties. Even more significantly, these 'long monomers' clearly differ in their physiological properties from short monomers lacking the neck. They have a much slower ATPase activity, which can be accelerated by proteolytic removal of parts of the neck domain, suggesting a possible inhibitory effect of the neck on the catalytic core.

The distinct characteristics of the fungal neck domain are also reflected in a specific sequence pattern (Figure 1). Sequence alignments of fungal and animal conventional kinesins show that fungal necks are strongly conserved and differ clearly from their animal counterparts. Whereas fungal kinesins lack the striking cluster of charged residues in the first third of animal necks, they exhibit a conserved sequence pattern in the centre of the neck

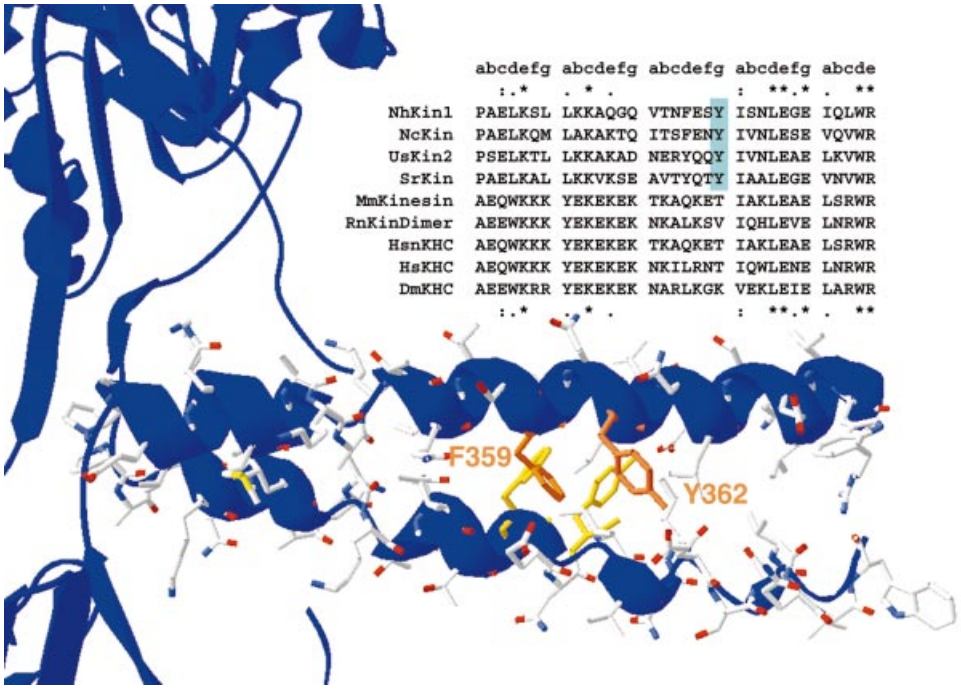


**Fig. 1.** Primary sequence and structural model of the kinesin neck domain. A sequence alignment of several conventional kinesin neck domains highlights the distinct and conserved sequence patterns of fungal and animal neck regions. The heptad structure of the coiled-coil is indicated above the alignment. In the first and last heptads, homology between fungal and animal kinesins is visible, indicated by asterisks for amino acid identity and dots for similarity. The central heptad of the neck clearly differs in fungi and animals. The Y362, highlighted in blue, is strictly conserved within all fungal kinesins but is not present in animals. In the lower part of the figure, the primary sequence of the NcKin neck is modelled into the crystal structure of the neck coiled-coil from rat conventional kinesin (3KIN). The aromatic residues F359 and Y362 are highlighted. Kinesins from: NcKin, *N.crassa*; UsKin2, *Ustilago maydis*; SrKin, *S.racemosum*; MmKin, *Mus musculus*; HsnKHC *Homo sapiens* KHC, neuronal isoform; HsKHC *H.sapiens* ubiquitous kinesin; DmKHC, *Drosophila melanogaster*; RnKinDimer, rat kinesin dimer.

(F/Y-E/Q-x-Y) which is not found in animal kinesins. The latter tyrosine (Y362 in NcKin), in particular, is strictly conserved among all known fungal kinesins, suggesting an important function.

Here we use a mutagenesis approach to study the role of the neck for motor function. Our results demonstrate that the exchange of Tyr 362 leads to a severely impaired motor which is unable to move at wild-type velocity. Without Y362, the neck domain is unable to form a two-stranded α-helical coiled-coil, leading to kinetically uncoupled heads. Unexpectedly, the mutation even increases the ATPase turnover of constructs that are monomeric in the wild-type background, indicating an inhibitory effect of the wild-type Y362 residue on the catalytic properties of the motor domain. Therefore in this work we demonstrate a direct role of the neck domain in regulation of the catalytic motor core, extending the previous view of the neck coiled-coil as a dimerization domain.

## Results

Fungal kinesins are unusually fast moving conventional kinesins (Steinberg and Schliwa, 1996). A conserved sequence pattern in fungal neck domains, which is distinct from the corresponding animal sequences, suggests an important role of the specific features of the fungal neck domain. Figure 1 shows a sequence comparison of the neck regions of various conventional kinesins. In fungal necks, a highly conserved tyrosine is found in position 362, which is not present in animal kinesins. To test the role of this tyrosine for motor functionality, it was exchanged against lysine, the corresponding residue of *Drosophila* conventional kinesin.

### *The point mutation Y362K uncouples ATP hydrolysis and movement of the motor*

The gliding velocities of bacterially expressed full-length (NcKin928) and truncated (NcKin433) forms of both wild-type and Y362K mutant variants were tested in a microscopic gliding assay. Because the truncated NcKin433 motors did not adhere to the glass surface, C-terminally cysteine-tagged versions of the constructs were biotinylated using biotin-maleimide and bound onto streptavidin-coated coverslips. Previous studies showed that the C-terminal cysteine tag does not change the catalytic and motile properties of the motor (Kallipolitou *et al*., 2001). Under multiple motor conditions (0.04–0.05 mg/ml, corresponding to ~250 000 motors/μm$^2$), all constructs showed sustained and uniform movement of the microtubules (Table I). The wild-type motors NcKin928-wt and NcKin433-wt produced similar microtubule gliding velocities of 2.6 ± 0.3 μm/s and 2.2 ± 0.2 μm/s, respectively. The point mutants Y362K were only about half as fast (1.1 ± 0.2 μm/s for NcKin928-Y362K, and 1.0 ± 0.2 μm/s for NcKin433-Y362K). *In vivo*, the full-length NcKin928-Y362K was unable to fully rescue the growth defect of the NcKin knockout strain (25% of wild-type growth rate), emphasizing the devastating effect of the point mutation.

**Table I.** Gliding velocities and steady state ATPase activities of NcKin wild-type and relevant mutants

| Construct | Gliding velocity (μm/s) | $k_{cat}$ ($s^{-1}$) | $K_{m,ATP}$ (μM) | Basal activity $k_0$ ($s^{-1}$) |
|---|---|---|---|---|
| NcKin433 (wild type) | 2.2 ± 0.2 | 74 ± 8 | 90 ± 13 | 0.017 ± 0.001 |
| NcKin433-Y362K | 1.0 ± 0.2 | 262 ± 7 | 90 ± 10 | 0.027 ± 0.000 |
| NcKin433-Y362C | –[a] | 176 ± 52 | ND | ND |
| NcKin433-Y362F | 1.6 ± 0.3 | 32 ± 15 | ND | ND |
| NcKin433-F359C | –[a] | 66 ± 31 | ND | ND |
| NcKin383 | 0.8 ± 0.2[b] | 24 ± 4[b] | ND | ND |
| NcKin383-Y362K | –[a] | 157 ± 0 | ND | ND |

The values are averages of at least two independent measurements.
[a]Biotinylation impossible.
[b]Data from Kallipolitou *et al*. (2001).

**Table II.** Oligomerization of NcKin and Y362 point mutants

| Construct | $S_{w,20}$ ($s^{-1}$) | $r_{Stokes}$ (nm) | Derived molecular mass (kDa) | Predicted mass from sequence (kDa) | Oligomerization state |
|---|---|---|---|---|---|
| NcKin433 | 4.3 | 4.7 | 83.4 | 47.9 | Dimer |
| NcKin433-Y362K | 3.3 | 4.0 | 54.5 | 47.9 | Monomer |
| NcKin433-Y362C | 3.6 | 3.8 | 56.5 | 47.9 | Monomer |
| NcKin433-Y362F | 3.5 | 3.7 | 53.5 | 47.9 | Monomer |
| NcKin433-F359C | 4.7 | 4.3 | 83.4 | 47.9 | Dimer |
| NcKin383 | 4.0 | 3.0 | 49.5 | 42.7 | Monomer |
| NcKin383-Y362K | 3.6 | 3.2 | 47.6 | 42.7 | Monomer |

Novel mutants were tested on two or three independent preparations.

To test whether this dramatic decrease of velocity was due to impaired ATP hydrolysis, we measured the steady state ATPase activities of the constructs using a coupled enzymatic assay (Table I). NcKin433-wt exhibits a $k_{cat}$ of 74 ± 8 $s^{-1}$, similar to the full-length protein. The mutant showed an extremely fast ATP turnover of 262 ± 7 $s^{-1}$, with similar values for the truncated and the full-length versions.

### *Specific requirement of tyrosine*

To determine whether the effect was specific for the introduced lysine, we replaced Y362 with cysteine and phenylalanine, respectively, and measured the steady state ATPase rates. The turnover of the Y362C mutant was comparable to that of the lysine mutant [$k_{cat}$ = 176 ± 52 $s^{-1}$ (average of 212 $s^{-1}$ and 139 $s^{-1}$ obtained for two independent preparations)], confirming that it is the absence of the tyrosine residue that results in a mutant phenotype. However, the effect seems to depend on the aromatic ring of tyrosine (rather than on its OH group) because the NcKin433-Y362F mutant shows a slow turnover comparable to that of the wild-type NcKin383 construct ($k_{cat}$ = 32 ± 15 $s^{-1}$).

To test whether a pi–pi stacking interaction of Y362 and F359 is required for proper neck functionality, we changed the other aromatic residue in the conserved fungal sequence motif (F359/Y-E/Q-x-Y) into cysteine. The $k_{cat}$ of the construct NcKin433-F359C varied from 44 to 88 $s^{-1}$, depending on the preparation, and thus did not show the extreme acceleration seen in the Y362 mutants. Apparently, this effect depends specifically on Tyr 362 and is not caused by the absence of any aromatic residue in the neck region.

To elucidate whether the acceleration of ATP hydrolysis in the Y362K point mutant was due to an intrinsically higher activity of the construct, the basal ATPase activities of wild-type and mutant NcKin433 in the absence of microtubules were measured (Table I). The basal ATP turnover rates differed less than those of wild-type constructs of different lengths (0.02–0.03 $s^{-1}$; Kallipolitou *et al*., 2001). Therefore the catalytic mechanism of the Y362K mutant seems to be unchanged, but the stimulation by microtubules is much more pronounced than in the case of the wild-type kinesin.

### *Oligomerization state of Y362 mutants*

The Y362K mutant with its accelerated ATPase but decreased gliding velocity is reminiscent of the monomeric NcKin construct lacking the neck and all subsequent domains (NcKin343; Kallipolitou *et al*., 2001). This construct also moves slowly ($v$ = 0.65 μm/s) and hydrolyses ATP at a similar rate ($k_{cat}$ = 260 $s^{-1}$). Therefore the oligomerization state of NcKin433-Y362K was assayed by gel filtration chromatography and sucrose density centrifugation (Table II). The deduced molecular masses indicate that, in contrast with the wild type, NcKin433-Y362K and Y362C are monomeric. It is noteworthy that the NcKin433-Y362F variant is also monomeric, suggesting a significant contribution of the OH group to the stabilization of the neck coiled-coil.

In agreement, cross-linking experiments with the double mutant NcKin433-P342C/Y362K failed to detect intersubunit interactions. Whereas the NcKin433-P342C single-point mutant oxidized by 5,5′ dithio-bis-(2-nitrobenzoic acid) (DTNB) runs as a dimer on a non-reducing sodium dodecyl sulfate (SDS) gel, the double mutant remains monomeric (Figure 2).

### Synthetic peptides

The dimerization characteristics of the Y362 mutants agree with data obtained for synthetic peptides. To study the effect of the Y362K mutation on dimerization, peptides of the NcKin neck region comprising residues 338–379 (Kn1/2) were synthesized (Table III) [the detailed study of the synthetic peptides is reported elsewhere (Deluca *et al*., 2002)]. Previous studies on synthetic wild-type peptide (Kn1) clearly revealed that the neck domain is able to fold into a coiled-coil only under acidic conditions (pH 3) (Kallipolitou *et al*., 2001). This coiled-coil conformation of the wild-type peptide Kn1 was well assessed by circular dichroism (CD) spectroscopy as the spectra displayed a ratio $[\Theta]_{222}/[\Theta]_{208}$ of 1.03. Further proof for this type of conformation was obtained from trifluoroethanol titration, thermal denaturation and mass spectrometry. Conversely, the corresponding mutant peptide Kn2 (Deluca *et al*., 2002) displays a CD spectrum at room temperature which is characteristic of an α-helical conformation with the two negative bands at 208 and 222 nm but with $[\Theta]_{222}/[\Theta]_{208} < 1$, which excludes the presence of a coiled-coil. This conformational state may be assumed by Kn2 at pH 3 and 5°C where $[\Theta]_{222}/[\Theta]_{208} > 1$. Thermal denaturation reveals a lower melting temperature compared with the wild-type peptide Kn1, suggesting a reduced coiled-coil stability.

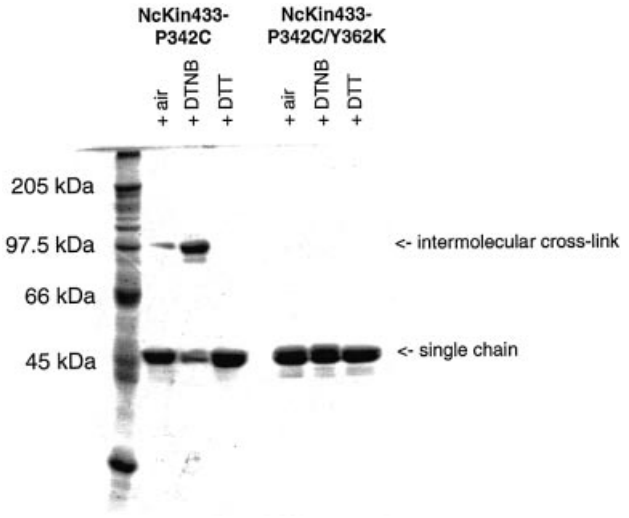


**Fig. 2.** Cross-linking NcKin433-P342C and NcKin433-P342C/Y362K. The mutants NcKin433-P342C and NcKin433-P342C/Y362K were fractionated on a non-reducing SDS gel. Under oxidizing conditions with 200 μM DTNB, most of the protein doubled its size (96 kDa), indicating an intermolecular cross-link. To a smaller extent, cross-links were formed by air oxidation. Under reducing conditions with 1 mM DTT, the disulfide bonds were broken and the protein appeared as a single chain (48 kDa). In the case of the double mutant NcKin433-P342C/Y362K, no dimerization could be observed under any conditions.

### The monomeric construct NcKin383-Y362K possesses higher catalytic activity than the monomeric wild type

Shorter mutant constructs show the same dimerization behaviour as NcKin433-Y362K and are also monomeric (Table II).

The NcKin383-Y362K mutant is of particular interest because the corresponding wild-type mutant is also monomeric, allowing kinetic comparisons that are unaffected by inter-head coordination of the wild-type version. Therefore we tested the kinetic properties of NcKin383-Y362K. Surprisingly, the steady state ATPase activitiy of this construct differs markedly from that of the corresponding wild-type construct (Table I). As observed previously, NcKin383-wt has a rather low $k_{cat}$ of 24 ± 4 $s^{-1}$ (Kallipolitou *et al*., 2001). However, the corresponding point mutant has a 6- to 7-fold accelerated turnover of 157 ± 0 $s^{-1}$. Also, the (monomeric) NcKin391-Y362K mutant clearly shows elevated ATPase activity (115 ± 15 $s^{-1}$). These findings suggest that Tyr 362 serves a dual function: it promotes dimerization of the neck, and it downregulates the ATP turnover of the motor core. To track down the kinetic step that is affected by Y362 we performed stopped-flow assays on NcKin383 wild-type and mutant variants.

### The Y362 mutation accelerates the mantADP release rate of NcKin

To follow the microtubule-dependent ADP release, we used the fluorescent ADP analogue *N*-methylanthranoyl-ADP (mantADP), which exhibits a higher fluorescence intensity when bound to a protein than when free in solution (Ma and Taylor, 1997a,b). NcKin was incubated with mantATP, which yields a kinesin–mantADP complex since ATP is hydrolysed quickly, even in the absence of microtubules. To validate the method, the stoichiometry of the mantADP release was assayed. NcKin–mantADP complexes were mixed in the fluorimeter first with microtubules and then with ATP. Figure 3A shows the change in the fluorescence signal when using wild-type NcKin433–mantADP complexes. On mixing with an excess of microtubules, the signal decreased to about half of its initial value (1.0), reflecting the release of mantADP from the first head. To prevent traces of ATP or GTP from starting off the cycle, 2 U/ml apyrase were present in the microtubule fraction. When ATP was added, the fluorescence signal decreased to a background level (0.0) of free mantADP in solution due to the release of mantADP from the second head. Figure 3B shows a titration experiment comparing NcKin433-wt–mantADP

**Table III.** Characteristics of synthetic neck peptides

| Peptide | Sequence | Melting temperature (°C) |
|---|---|---|
| Kn1 | Ac-A-E-L-S-P-A-E-L-K-Q-M-L-A-K-A-K-T-Q-I-T-S-F-E-N-Y-I-V-N-L-E-S-E-V-Q-V-W-R-G-G-E-T-V-$NH_2$ | 47.2 |
| Kn2 | Ac-A-E-L-S-P-A-E-L-K-Q-M-L-A-K-A-K-T-Q-I-T-S-F-E-N-K-I-V-N-L-E-S-E-V-Q-V-W-R-G-G-E-T-V-$NH_2$ | 19.6 |

Deluca *et al*. (2002).

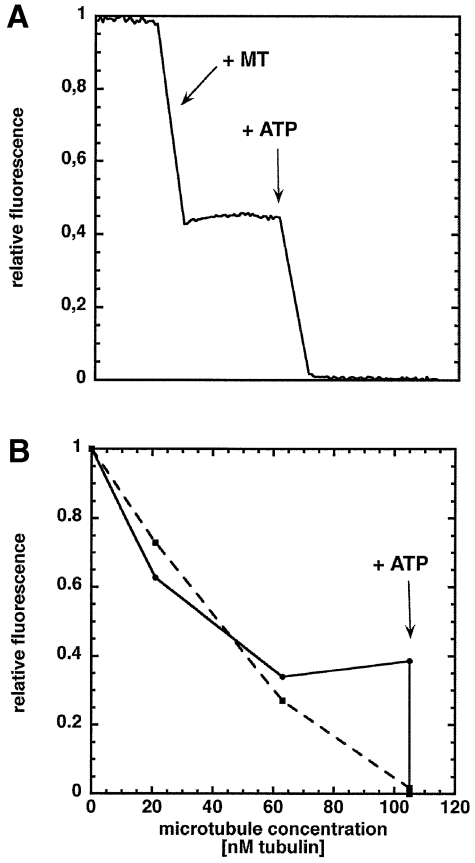


**Fig. 3.** Stoichiometry of the microtubule-activated mantADP release from NcKin433-wt and NcKin433-Y362K. MantADP-loaded NcKin (100–250 nM) was mixed with microtubules to follow the ADP release. (**A**) At equimolar amounts of microtubules, the signal reaches a plateau at 0.4, indicating the release of ~60% of the mantADP. After adding 1 mM ATP, the residual mantADP is released and the signal decreases to the background level of free mantADP in solution. (**B**) Titration of NcKin433-wt–mantADP and NcKin433-Y362K–mantADP complexes with microtubules (solid line and circles, NcKin433-wt–mantADP; broken line and squares, NcKin433-Y362K–mantADP). In contrast with the wild type, the mutant releases all its mantADP upon microtubule binding without ATP, indicating uncoupled heads.

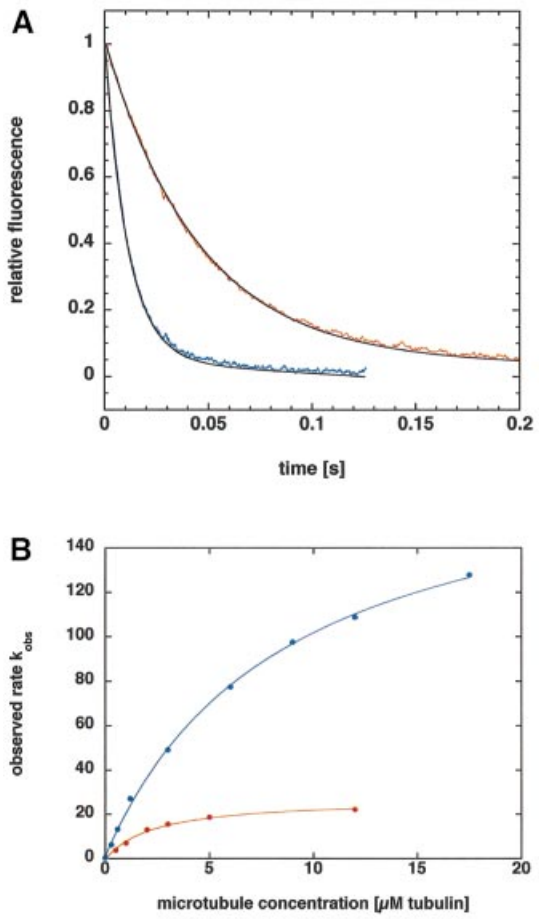


**Fig. 4.** Pre-steady state kinetics of mantADP release from NcKin383–mantADP complexes: (A) shows example traces of mantADP release from wild-type and mutant NcKin383, and (B) shows the dependence of release rates from microtubule concentration. (**A**) Two examples of stopped-flow traces monitored by mixing 0.2–0.3 μM NcKin383-wt–mantADP (red curve) and NcKin383-Y362K–mantADP (blue curve) complexes with 6 μM microtubules in the presence of 2 mM ATP. The traces are averages of 3 to 5 single transients. The black curves are fits to a single-exponential equation. (**B**) The observed rates $k_{obs}$ for one example of wild type (red) and one example of the Y362K mutant (blue) plotted against the microtubule concentration show a hyperbolic dependence. The average of three independent measurements yields maximum rates of 29 ± 3 $s^{-1}$ for wild-type NcKin383 and 191 ± 34 $s^{-1}$ for the mutant.

and 433-Y362K–mantADP complexes. Microtubules were added in small aliquots until stoichiometric amounts were reached. For both constructs the fluorescence decreased markedly. In the case of NcKin433-wt–mantADP, the signal reached a plateau, reflecting the binding of the first head. The observation that >50% of the mantADP is released may be due to a small extent of mantADP dissociation from the second head (Ma and Taylor, 1997a). In agreement with the monomeric state of the mutant protein, addition of microtubules to mantADP-labelled NcKin433-Y362K led to an ATP-independent decrease of the fluorescence signal to background levels, and was not altered further by addition of ATP.

To assess microtubule binding and mantADP release kinetics, the monomeric NcKin383-wt–mantADP complex was mixed with varying microtubule concentrations in the stopped-flow instrument in the presence of 2 mM ATP (Figure 4). The traces could be fitted by single-exponential equations. The apparent rates $k_{obs}$ extrapolated to a maximum $k_{max}$ of 29 ± 3 $s^{-1}$ (Table IV), similar to $k_{cat}$ (24 $s^{-1}$). The microtubule-stimulated mantADP release of mutant NcKin383-Y362K also obeyed single-exponential dependence at all microtubule concentrations, but extrapolated to a 6.6-fold faster $k_{max}$ (191 ± 34 $s^{-1}$). The $k_{cat}$ of this construct (157 $s^{-1}$) is accelerated by a factor of 6.5, suggesting that the inhibition by Y362 acts on the level of the ADP release step. The half-maximal activation constants were 3.9 ± 1.4 μM (wild type) and 7.7 ± 2.4 μM (Y362K), respectively.

**Table IV.** Pre-steady state kinetics of the mantADP release

| NcKin383 | | NcKin383-Y362K | |
|---|---|---|---|
| $k_{max}$ ($s^{-1}$) | $K_{0.5,Mt}$ (μM) | $k_{max}$ ($s^{-1}$) | $K_{0.5,Mt}$ (μM) |
| 29 ± 3 | 3.9 ± 1.4 | 191 ± 34 | 7.7 ± 2.4 |

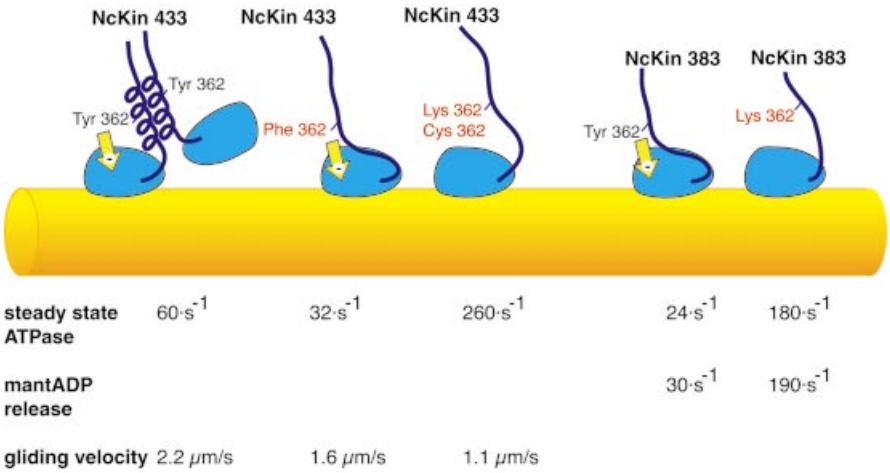


**Fig. 5.** Possible functions of Y362. Schematic representation of the dual function of Y362. In the dimeric background (NcKin433, left) the mutation leads to a disruption of the neck coiled coil, resulting in a fast ATPase rate and a slow gliding velocity. In the monomeric wild-type background (NcKin383, right) Y362 mediates an interaction of the unfolded neck domain with the motor core which represses the ATPase activity (yellow arrow). The K362 substitution is unable to regulate the core motor domain, which catalyses a fast ATP turnover comparable to the truncated NcKin433 lacking the entire neck domain. The accelerated mantADP release rate in Y362K monomers indicates that the residue Y362 is involved in modulating the microtubule-activated ADP release.

## Discussion

Kinesins are microtubule-activated ATPases with a catalytic domain conserved within the entire superfamily of kinesin-related proteins (Vale and Fletterick, 1997; Woehlke and Schliwa, 2000). In addition, the family of conventional kinesins possesses an essential, structurally conserved coiled-coil neck domain that helps to dimerize the two heads of the motor. The neck domain is involved in translating the energy derived from ATP hydrolysis in the motor core into processive movement, but its precise role is poorly understood.

Here, we have studied the fungal neck domain in a detailed analysis of NcKin mutants by addressing a highly conserved tyrosine at position 362. The motile and ATPase characteristics of NcKin433-Y362K exhibited striking differences when compared with the wild-type construct NcKin433-wt: $k_{cat}$ was enhanced 3- to 4-fold, whereas the velocity in a multiple motor gliding assay was less than half that of the wild-type. This dramatic effect of the exchange of one amino acid residue in the neck resembles the consequences of the deletion of the entire neck domain of the *S.racemosum* kinesin (Grummt *et al*., 1998). As in the NcKin-Y362K point mutant, a 5-fold acceleration of the ATPase and a 2- to 3-fold reduction of the gliding velocity was observed. This amazing similarity hints at the prime importance of residue Y362 for proper neck functionality, in particular the effective coupling of ATP hydrolysis and movement of the motor. The basically identical basal ATP turnover rates of mutant and wild-type protein indicate that differences in motor functionality of the mutant are not intrinsic to the protein but are manifested in their interaction with the microtubule.

At first sight, the defect caused by mutation of Y362 is due to a defective neck coiled-coil. The failure of NcKin433 to dimerize when Y362 is exchanged shows that the interaction within the dimer is weakened in the mutant protein. Also, data from peptide studies indicate a lower coiled-coil propensity for the mutant peptides. Moreover, the inter-subunit cross-link between two cysteines in the neck domain is only possible with the wild-type Y362.

The effect of the Tyr substitution on the dimerization behaviour does not depend on whether a Lys or Cys is introduced. The vicinity of the conserved aromatic residue F359 suggested that Y362 and F359 may form stacking interactions (Figure 1). However, the F359C mutant is still dimeric. In contrast, the mutant Y362F which does retain the aromatic side-chain is monomeric. Thus, stacking interactions are not relevant for coiled-coil stabilization, but the OH group seems to be required. As Tyr is usually uncharged in proteins, stabilizing salt bridges are unlikely. However, the exact mechanism by which Y362 enhances the coiled-coil propensity remains unclear.

A closer look at the effect of the Y362 exchanges reveals a more complex situation and suggests a second important role in addition to coiled-coil stabilization. Our results on NcKin variants that are dimeric as wild-type protein but monomeric as mutant (NcKin433) explain the dramatic effects of the point mutation as a consequence of a lack of head–head interaction, as required by the alternating-head model of kinesin function. However, as indicated by the ATPase characteristics of the shorter mutant constructs, stabilization of the neck structure is not the only function of Tyr 362. The ATP turnover of all Y362K/C mutants is accelerated up to 7-fold compared with their respective wild-type constructs (Table I). That Y362 does not only stabilize the α-helical neck coiled coil is also supported by the Y362F mutation; it disrupts dimerization of NcKin433 but does not lead to an accelerated ATPase rate.

The simplest explanation for these observations is an inhibitory effect of the neck on the ATPase activity of the catalytic core, mediated by residue Y362 (Figure 5). While the wild-type neck slows down the ATPase rate from 260 to 24 $s^{-1}$, the mutant lacking the crucial tyrosine residue is

unable to modulate the motor head and thus shows a comparable rate as the neckless deletion mutant. As indicated by comparison of Y362K/C and Y362F mutants, the aromatic ring of tyrosine may be sufficient to regulate the ATPase activity, whereas the hydrophilic OH group is necessary for proper coiled-coil interstrand interaction. Previous mapping studies of the NcKin motor revealed that monomeric constructs comprising the neck domain are 10-fold slower than the motor core without a neck (Kallipolitou *et al*., 2001). After proteolytic removal of residues from the neck domain the ATP turnover was accelerated. These data are in agreement with the present study and strongly support the conclusion that the neck domain is able to repress the catalytic activity of the core motor domain.

Regardless of the exact structural basis of the inhibition, our mantADP release experiments indicate that Y362 slows down the microtubule-activated ADP release. In the mutant NcKin383-Y362K, the ADP release is 6- to 7-fold faster than in the wild type. Strictly, we cannot exclude the possibility that other kinetic steps are accelerated, but the mutant's mantADP release rate is increased by as much as the steady state rate and thus is sufficient to explain the effect fully. Moreover, the similar $K_{m,ATP}$ of the wild type and the mutant suggests similar ATP on and off rates (Table I). It has been shown that the tail inhibition mechanism for *Drosophila* kinesin involves a slowdown of ADP release (Hackney and Stock, 2000). Therefore we can speculate that, in the physiological case, Y362 mediates the regulatory influence of the tail region, which has been shown to downregulate the ATPase activity (Coy *et al*., 1999; Friedman and Vale, 1999; Seiler *et al*., 2000).

In conclusion, this work demonstrates for the first time a direct influence of the conventional kinesin neck domain on the regulation of the microtubule-dependent ATPase activity. Thus, we show that kinesin's neck can exert a direct action via Y362 on the motor behaviour, as opposed to a passive indirect action imposed by its influence on kinesin dimerization. Because monomeric constructs including the neck region of animal conventional kinesins do not exist, this regulatory influence of the neck domain previously remained undetected. Moreover, as Y362 is specifically conserved in fungal kinesins, regulation in animal conventional kinesins may involve different protein regions. Identifying these regions will help to determine whether animal conventional kinesins possess a similar regulatory mechanism.

## Materials and methods

### Cloning and expression

Initially, the Y362K point mutation was introduced into the full-length bacterial clone pT12.1 (Henningsen and Schliwa, 1997). Subsequent truncated versions of the motor were generated from pT12.1-Y362K by the polymerase chain reaction (PCR) (Kallipolitou *et al*., 2001). The exchanges Y362C, F359C and P342C were introduced using the Quickchange protocol (Stratagene Inc.). For fungal expression, a suitable restriction fragment from pT12.1-Y362K was transferred into the fungal expression vector p43Nkin (Kirchner *et al*., 1999; Seiler *et al*., 2000).

To express NcKin protein, media flasks containing 2 l TPM (20 g/l tryptone, 15 g/l yeast extract, 2.5 g/l $Na_2HPO_4$, 1.0 g/l $NaH_2PO_4$, 10 mM glucose, 100 µg/ml ampicillin) were inoculated from a freshly transformed single colony of *Escherichia coli* BL21 CodonPlus (DE3)-RIL (Stratagene Inc.). Cells were pregrown for 16–20 h at 22 or 37°C, induced with 1 mM ispropyl-β-D-thiogalactopyranoside (IPTG) and incubated overnight at 22°C. Cells were harvested the next morning and stored at –70°C.

Purification was accomplished as described (Crevel *et al*., 1999). Briefly, 4 g of *E.coli* cells were resuspended in buffer A [20 mM Na phosphate pH 7.4, 50 mM NaCl, 5 mM $MgCl_2$, 1 mM EGTA, 1 mM dithiothreitol (DTT), 10 µM ATP, protease inhibitor mix (Roche Diagnostics)], sonicated and centrifuged (35 min at 100 000 *g*). The supernatant was loaded on a 5 ml HiTrap SP Sepharose column (Amersham Pharmacia Biotech) and eluted without DTT in a manual NaCl step gradient. The peak fractions were pooled, frozen in liquid nitrogen with 10% glycerol and stored at –70°C. Protein concentrations were evaluated by a Bradford assay.

### Size determination

To characterize the oligomerization state of NcKin constructs, the molecular weights were estimated by gel filtration chromatography and sucrose density centrifugation as described previously (Kallipolitou *et al*., 2001).

### Labelling of reactive cysteine tags

The cysteine-tagged NcKin433 constructs were labelled with biotin–maleimide (Kallipolitou *et al*., 2001). The protein was incubated with a 6-fold molar excess of maleimide conjugate on ice for 60 min. The reaction was stopped with 10 mM DTT. Active kinesin was isolated by a microtubule binding and release step (Vale *et al*., 1985).

### Gliding assays

Motility assays were performed with biotin-labelled kinesins in flow cells coated with streptavidin (Kallipolitou *et al*., 2001). After incubation for 5 min [1 mg/ml streptavidin (Sigma Chemical Corp.) in BRB80+ (80 mM PIPES–KOH pH 6.8, 1 mM $MgCl_2$, 1 mM EGTA, 5 mM Mg-acetate)], the cells were washed with three chamber volumes of blocking buffer (1 mg/ml bovine serum albumin, 0.8 mg/ml casein in BRB80+) and filled with biotin-labelled kinesin in blocking buffer (20–30 µM). After 10 min incubation the assays were started by floating the cells with motility buffer (10 mM $MgCl_2$, 10 mM ATP, 200 mM KCl, 20 µM paclitaxel and microtubules in BRB80+). The $K_{m,ATP}$ (motility) was measured by floating one cell several times with motility buffer containing increasing amounts of ATP. Gliding of the microtubules was monitored in a Zeiss Axiophot using video-enhanced phase-contrast microscopy.

### Steady state microtubule ATPase activity

Steady state ATPase rates were determined using a coupled enzymatic assay (Grummt *et al*., 1998; Huang and Hackney, 1994a). The assays were performed in the low ionic strength buffer 12A25+ [standard ATPase buffer: 12 mM *N*-[2-acetamido]-2-aminoethanesulfonic acid (ACES)–KOH pH 6.8, 25 mM K-acetate, 2 mM Mg-acetate, 0.5 mM EGTA, 3 mM $MgCl_2$]. Reactions were started by adding kinesin. For determining steady state kinetics as a function of the microtubule concentration, ATP was used at a saturating concentration of 1 mM. The $K_{m,ATP}$ (ATPase) was measured at a constant saturating microtubule concentration (2 µM for 433-wt; 10 µM for 433-Y362K) and various ATP concentrations.

Microtubules from pig brain tubulin (Mandelkow *et al*., 1985) were polymerized freshly from pre-spun tubulin, stabilized with 20 µM paclitaxel and recentrifuged to remove excess nucleotide. The concentration of the resuspended microtubule solution was determined photometrically at 280 nm (Huang and Hackney, 1994b).

### Basal ATPase measurements

The ATPase rates in the absence of microtubules were measured by following the phosphate release using a malachite green reagent for colorimetric detection of phosphate (Geladopoulos *et al*., 1991).

The assays were started by adding NcKin at 0.3 and 0.6 µM to 1 mM ATP in 12A25+, alongside a blank without kinesin. The reactions were stopped after 10 s, 20 s, 30 s, 1 min, 2 min, 5 min and 30 min in 0.3 M perchloric acid. The malachite green reagent [0.3 g/l malachite green (Sigma Chemicals Corporation), 2 g/l Na-molybdate and 0.5 g/l Triton X-100 in 0.7 M HCl, filtered and stored at 4°C] was added and the phosphate concentrations were determined after 15 min by comparison with an appropriate $NaH_2PO_4$ standard. The basal ATPase rates were calculated from fits to the linear part of time traces.

### Fluorimetric measurements of the mantADP release

To charge NcKin with mantADP, the kinesin constructs were incubated with a 3-fold molar excess of mantATP at 25°C for 15 min. The

kinesin–mantADP complexes were separated from excess nucleotide via Sephadex G25 spin columns. The protein concentration and the labelling ratio were determined by measuring absorption at 280 and 356 nm (extinction coefficients: NcKin433-wt, 29 170 $cm^{-1}M^{-1}$; NcKin433-Y362K, 22 200 $cm^{-1}M^{-1}$; manthranoyl group, 5800 $cm^{-1}$ $M^{-1}$). Labelling ratios of about 80–100% were usually achieved.

Kinesin–microtubule binding was monitored via the release of mantADP in an Aminco Bowman spectrofluorimeter (Ma and Taylor, 1997a; Kallipolitou *et al*., 2001). All assays were performed at 22°C in standard ATPase buffer 12A25+. The excitation wavelength was 365 nm and the emitted fluorescence was monitored at 445 nm. Then, 100–250 nM of kinesin–mantADP complexes were mixed with at least equimolar amounts of microtubules (0.1–1 μM end concentration) either by adding them completely or in small aliquots. Microtubule preparations contained 2 U/ml apyrase to remove traces of ATP or GTP. The decrease of fluorescence was monitored in a time course or by noting the signal after each addition. To release the second mantADP, an excess of ATP (1–2 mM) was subsequently added.

### *Stopped-flow measurements of the mantADP release*

Pre-steady state kinetics of mantADP release were measured in a BioLogic stopped-flow apparatus (SFM-3). All assays were performed at 22°C in 12A25+. All traces shown represent the average of three to five stopped-flow traces. An excitation wavelength of 365 nm was used, and emission was monitored using a narrow-band interference filter with a slit width of 442 ± 10 nm.

To determine mantADP release rates, 200–300 nM of kinesin–mantADP complexes (all concentrations are final concentrations) was rapidly mixed with 0–18 μM microtubules in the presence of 2 mM ATP. All traces could be fitted to single exponentials using the software BioKine (BioLogic). The rates showed a hyperbolic dependence on the microtubule concentration and could be fitted to the hyperbolic equation

$$y = B + k_{max}[Mt]/([Mt] + K_{0.5,Mt})$$

The results are averages from three independent experiments.

### *Peptide synthesis*

The peptides Kn1 and Kn2 were synthesized automatically by solid-phase Fmoc/tBu chemistry as described (Kallipolitou *et al*., 2001).

### *Circular dichroism*

The CD spectra were recorded on a Jasco J-715 spectropolarimeter at 20°C using quartz cuvettes and a temperature controller PFD-350S. The concentration of the filtered samples (0.45 μm) was determined by absorbance at 280 nm. The spectra (average of 10 scans) were normalized to their mean residue molar ellipticity $[\Theta]_R$ (deg $cm^2$/dmol). The spectra were recorded between 185 and 250 nm with a scanning speed of 50 nm/min, a response of 1 s and a bandwidth of 1 nm. Melting curves were measured by following the change in the ellipticity at 222 nm with temperature, with a temperature slope of 30°C/h, a response time of 16 s and a bandwidth of 1 nm.

### *Chemical cross-linking*

Reversible disulfide-bonds were formed between the two cysteines of dimeric NcKin433-P342C by incubation with DTNB or air (Tomishige and Vale, 2000). First, 200 μM of DTNB, dissolved in dimethylsulfoxide, was added to 20–50 μM NcKin433-P342C or NcKin433-Y362K, P342C and incubated for 15 min. Then SDS-sample buffer without reducing reagents was added. To verify air-oxidation, non-incubated kinesin constructs were mixed with sample buffer. Disulfide bonds were broken by reduction with DTT. Next, 1 mM DTT was added to 20–50 μM kinesin, incubated for another 15 min and then mixed with SDS-sample buffer. SDS–PAGE was performed with all samples, followed by Coomassie Blue staining.

## Acknowledgements

We thank Dr W.Heinzel for help with the peptide synthesis and Judith Mergler and Katrin Hahlen for assistance during the revision. F.S. acknowledges support from the EMBO workshop 'The application of transient kinetics to biological macromolecules' (Professor M.Geeves). This work is supported by grants SFB 413 and SPP 1068 from the Deutsche Forschungsgemeinschaft.

## References

Coy,D.L., Hancock,W.O., Wagenbach,M. and Howard,J. (1999) Kinesin's tail domain is an inhibitory regulator of the motor domain. *Nat. Cell Biol.*, **1**, 1465–7392.

Crevel,I., Carter,N., Schliwa,M. and Cross,R. (1999) Coupled chemical and mechanical reaction steps in a processive *Neurospora* kinesin. *EMBO J.*, **18**, 5863–5872.

Deluca,D., Woehlke,G. and Moroder,L. (2002) Synthesis and conformational characterization of peptides related to the neck of a fungal conventional kinesin. *J. Pept. Sci.*, in press.

Friedman,D.S. and Vale,R.D. (1999) Single-molecule analysis of kinesin motility reveals regulation by the cargo-binding tail domain. *Nat. Cell Biol.*, **1**, 1465–7392.

Geladopoulos,T.P., Sotiroudis,T.G. and Evangelopoulos,A.E. (1991) A malachite green colorimetric assay for protein phosphate activity. *Anal. Biochem.*, **192**, 112–116.

Grummt,M., Woehlke,G., Henningsen,U., Fuchs,S., Schleicher,M. and Schliwa,M. (1998) Importance of a flexible hinge near the motor domain in kinesin-driven motility. *EMBO J.*, **17**, 5536–5542.

Hackney,D.D. and Stock,M.F. (2000) Kinesin's IAK tail domain inhibits initial microtubule-stimulated ADP release. *Nat. Cell Biol.*, **2**, 257–260.

Hancock,W.O. and Howard,J. (1999) Kinesin's processivity results from mechanical and chemical coordination between the ATP hydrolysis cycles of the two motor domains. *Proc. Natl Acad. Sci. USA*, **96**, 13147–13152.

Henningsen,U. and Schliwa,M. (1997) Reversal in the direction of movement of a molecular motor. *Nature*, **389**, 93–96.

Huang,T. and Hackney,D. (1994a) *Drosophila* kinesin minimal motor domain expressed in *Escherichia coli*. Purification and kinetic characterization. *J. Biol. Chem.*, **269**, 16493–16501.

Huang,T.G. and Hackney,D.D. (1994b) *Drosophila* kinesin minimal motor domain expressed in *Escherichia coli*. Purification and kinetic characterization. *J. Biol. Chem.*, **269**, 16493–16501.

Huang,T., Suhan,J. and Hackney,D. (1994) *Drosophila* kinesin motor domain extending to amino acid position 392 is dimeric when expressed in *Escherichia coli*. *J. Biol. Chem.*, **269**, 16502–16507.

Jiang,W. and Hackney,D.D. (1997) Monomeric kinesin head domains hydrolyze multiple ATP molecules before release from a microtubule. *J. Biol. Chem.*, **272**, 5616–5621.

Jiang,W., Stock,M.F., Li,X. and Hackney,D.D. (1997) Influence of the kinesin neck domain on dimerization and ATPase kinetics. *J. Biol. Chem.*, **272**, 7626–7632.

Kallipolitou,A., Deluca,D., Majdic,U., Lakamper,S., Cross,R., Meyhofer,E., Moroder,L., Schliwa,M. and Woehlke,G. (2001) Unusual properties of the fungal conventional kinesin neck domain from *Neurospora crassa*. *EMBO J.*, **20**, 6226–6235.

Kirchner,J., Seiler,S., Fuchs,S. and Schliwa,M. (1999) Functional anatomy of the kinesin molecule *in vivo*. *EMBO J.*, **18**, 4404–4413.

Kozielski,F., Sack,S., Marx,A., Thormahlen,M., Schonbrunn,E., Biou,V., Thompson,A., Mandelkow,E.M. and Mandelkow,E. (1997) The crystal structure of dimeric kinesin and implications for microtubule-dependent motility. *Cell*, **91**, 985–994.

Ma,Y.Z. and Taylor,E.W. (1997a) Interacting head mechanism of microtubule-kinesin ATPase. *J. Biol. Chem.*, **272**, 724–730.

Ma,Y.Z. and Taylor,E.W. (1997b) Kinetic mechanism of a monomeric kinesin construct. *J. Biol. Chem.*, **272**, 717–723.

Mandelkow,E.-M., Herrmann,M. and Rühl,U. (1985) Tubulin domains probed by limited proteolysis and subunit-specific antibodies. *J. Mol. Biol.*, **185**, 311–327.

Romberg,L., Pierce,D.W. and Vale,R.D. (1998) Role of the kinesin neck region in processive microtubule-based motility. *J. Cell Biol.*, **140**, 1407–1416.

Seiler,S., Kirchner,J., Horn,C., Kallipolitou,A., Woehlke,G. and Schliwa,M. (2000) Cargo binding and regulatory sites in the tail of fungal conventional kinesin. *Nat. Cell Biol.*, **2**, 333–338.

Steinberg,G. (1998) Organelle transport and molecular motors in fungi. *Fungal Genet. Biol.*, **24**, 161–177.

Steinberg,G. and Schliwa,M. (1996) Characterization of the biophysical and motility properties of kinesin from the fungus *Neurospora crassa*. *J. Biol. Chem.*, **271**, 7516–7521.

Thorn,K.S., Ubersax,J.A. and Vale,R.D. (2000) Engineering the processive run length of the kinesin motor. *J. Cell Biol.*, **151**, 1093–1100.

Tomishige,M. and Vale,R.D. (2000) Controlling kinesin by reversible disulfide cross-linking. Identifying the motility-producing conformational change. *J. Cell Biol.*, **151**, 1081–1092.

Vale,R.D. and Fletterick,R.J. (1997) The design plan of kinesin motors. *Annu. Rev. Cell. Dev. Biol.*, **13**, 745–777.

Vale,R.D., Reese,T.S. and Sheetz,M.P. (1985) Identification of a novel force-generating protein, kinesin, involved in microtubule-based motility. *Cell*, **42**, 39–50.

Woehlke,G. and Schliwa,M. (2000) Walking on two heads: the many talents of kinesin. *Nat. Rev. Mol. Cell Biol.*, **1**, 50–58.

Young,E.C., Mahtani,H.K. and Gelles,J. (1998) One-headed kinesin derivatives move by a nonprocessive, low-duty ratio mechanism unlike that of two-headed kinesin. *Biochemistry*, **37**, 3467–3479.

*Received May 24, 2002; revised October 14, 2002; accepted November 22, 2002*